

# A nanocarbon paste electrode modified with nitrogen-doped graphene for square wave anodic stripping voltammetric determination of trace lead and cadmium

Xinsheng Liu<sup>1</sup> · Zhaojun Li<sup>2</sup> · Runmei Ding<sup>1</sup> · Binbin Ren<sup>3</sup> · Yonghong Li<sup>3</sup>

Received: 10 September 2015 / Accepted: 3 December 2015 / Published online: 15 December 2015  
© Springer-Verlag Wien 2015

**Abstract** A nano-carbon paste electrode was modified with nitrogen doped graphene and applied to square wave anodic stripping voltammetric determination of lead(II) and cadmium(II). The modified electrode was investigated by cyclic voltammetry and electrochemical impedance spectroscopy. Key parameters affecting the performance of the sensor such as pH value, content of modifier, deposition potential and time were optimized. Under optimized conditions, the electrode exhibits linear response to lead (at about  $-0.56$  V) and cadmium (at about  $-0.77$  V) in the range between 10 pM to 1 nM, and the detection limits are 8.0 pM for cadmium(II) and 5.0 pM for lead(II), respectively. The sensitivity, selectivity and simplicity of the method are comparable to, or even better than those reported earlier.

**Keywords** Electrochemical impedance spectroscopy · Cyclic voltammetry · Nyquist plot · Hexacyanoferrate · Lake water analysis

**Electronic supplementary material** The online version of this article (doi:10.1007/s00604-015-1713-3) contains supplementary material, which is available to authorized users.

✉ Xinsheng Liu  
lxs21230@163.com

✉ Yonghong Li  
yonghongli2012@163.com

<sup>1</sup> School of Basic Medical Sciences, Ningxia Medical University, Yinchuan 750004, People's Republic of China

<sup>2</sup> School of Nursing, Ningxia Medical University, Yinchuan 750004, People's Republic of China

<sup>3</sup> Electrochemistry and Spectroscopy Analysis Laboratory, School of Public Health and Management, Ningxia Medical University, Yinchuan 750004, People's Republic of China

## Introduction

The heavy metals widely exist in the industrial processes of electroplating, batteries, papermaking and paint [1]. Lead ( $Pb^{2+}$ ) and cadmium ( $Cd^{2+}$ ) are toxic heavy metals, and their pollution is one of the serious environmental problems.  $Pb^{2+}$  and  $Cd^{2+}$  are non-biodegradability, and they can be accumulated in the human body during the long-term process, resulting in serious disorders to human organs [2, 3]. Thus, the trace quantification determination of  $Pb^{2+}$  and  $Cd^{2+}$  can provide important information for human health and environmental monitoring.

Some spectroscopic techniques have been utilized for the determination of lead and cadmium [4–6], those methods require specialized operator, sophisticated and expensive devices, and they are not appropriate for field measurement [7]. In contrast, electrochemical methods are proved to be easily operated, low-cost, rapid and portable [3, 8]. Initially, mercury based electrodes combined with anodic stripping voltammetry (ASV) are used for trace heavy metals analysis. The environmental friendly electrodes have gradually replaced the mercury-modified electrodes due to the high toxicity of mercury. They exhibit low toxicity, simple preparation, good sensitivity and selectivity. We used the chemically modified nano-carbon paste electrodes for the determination of  $Pb^{2+}$  and  $Cd^{2+}$ .

Various green electrode modification materials are utilized for improving electrochemical performance. Graphene is a two-dimensional single atom thick of  $sp^2$ -hybridized carbon material, and it exhibits excellent electrical conductivity, high mechanical strength, large surface area, and rapid heterogeneous electron transfer [9, 10]. Therefore, graphene plays an important role in the field of electrochemistry. Comparing with graphene, the properties of nitrogen-doped graphene (N-GE) have been further improved, including better electric

conductivity and enhanced electrocatalytic activity [11, 12]. Nitrogen-doped nanomaterials have great potential for preparing the electrochemical sensors. For example, Shi et al. [13] prepared an enzymeless  $\text{H}_2\text{O}_2$  sensor based on nitrogen-doped graphene nanoribbons modified electrode. The nano-modified electrode exhibited enhanced electron transfer ability, and possessed a large active surface and a large number of catalytically active sites that originated from the presence of nitrogen atoms. Giribabu et al. [14] utilized a nitrogen doped reduced graphene oxide modified glassy carbon electrode (GCE) for electrochemical sensing of 4-nitrophenol. Due to the electrocatalytic property of nitrogen doped reduced graphene oxide, the oxidation peak current of 4-nitrophenol improved significantly on the modified GCE compared to bare GCE. Tsierkezos et al. [15] fabricated pristine multi-walled carbon nanotubes (MWCNTs) and nitrogen-doped MWCNTs (N-MWCNTs) decorated with gold nanoparticles (AuNPs). N-MWCNTs/AuNPs exhibited better electrochemical response towards simultaneous oxidation of ascorbic acid (AA), uric acid (UA), and dopamine (DA) compared to that of MWCNTs/AuNPs. This was due to the presence of nitrogen that enhanced the electrocatalytic activity of MWCNTs.

We fabricated nano-carbon paste electrode using nano-graphite powder instead of common graphite powder. Compared with traditional carbon paste electrode (CPE), nano-carbon paste electrode (nano-CPE) revealed lower impedance and faster electron transfer. Then nitrogen-doped graphene was used to modify nano-carbon paste electrode for trace analysis of  $\text{Pb}^{2+}$  and  $\text{Cd}^{2+}$ . The electrochemical properties of the modified electrodes were evaluated by cyclic voltammetry and electrochemical impedance spectroscopy. Due to large surface area and good electrocatalytic activity of nitrogen-doped graphene, the modified nano-carbon paste electrode exhibited a remarkably improved sensitivity for  $\text{Pb}^{2+}$  and  $\text{Cd}^{2+}$  using square wave anodic stripping voltammetry. The method was applied for the determination of  $\text{Pb}^{2+}$  and  $\text{Cd}^{2+}$  in real samples.

## Experimental

### Reagents and materials

Graphite powder (spectrographic grade), paraffin oil, lead nitrate and cadmium nitrate were obtained from Sinopharm Chemical Reagent Co., Ltd. (Shanghai, China, <http://www.sinoreagent.com/>). Nano-graphite powder (thickness: <40 nm, sheet size: about 400 nm), plain graphene and nitrogen-doped graphene (nitrogen content: 3.0 wt% ~ 5.0 wt%; surface area: >500  $\text{m}^2/\text{g}$ ) were purchased from Nanjing XFNANO Materials Tech Co., Ltd. (Nanjing, China, <http://www.xfnano.com/>). Stock standard solutions of 2.5 mM  $\text{Cd}^{2+}$  and 2.5 mM  $\text{Pb}^{2+}$  were prepared by dissolution

of corresponding nitrate salts and working standard solutions were obtained by appropriate dilution. 0.2 M acetate buffer with various pH values were used as the supporting electrolytes. All other reagents were of analytical grade, and were used without further purification.

### Apparatus

All electrochemical measurements (except electrochemical impedance spectroscopy measurements) were performed using a CHI660E electrochemical workstation (Shanghai Chenhua Instruments Corporation, Shanghai, China, <http://www.chinstr.com/>). The electrochemical impedance spectroscopy (EIS) measurements were carried by a PARSTAT 4000 (Princeton Applied Research, America, <http://www.par-solartron.com.cn/>). A three electrode system was used containing a nitrogen doped graphene modified nano-carbon paste electrode (3.0 mm in diameter) as working electrode, a platinum wire as auxiliary electrode, and a saturated calomel electrode (SCE) as reference electrode. All potentials were reported with respect to the reference electrode. A KMO2 basic magnetic stirrer (IKA, Germany, <http://www.ika.cn/>) was used to stir the testing solution before measurements. All the experiments were carried out at room temperature.

### Electrode preparation

The nitrogen doped graphene modified nano-carbon paste electrode was prepared by the following procedures: A certain proportion of nano-graphite powder, nitrogen doped graphene, and paraffin oil were mixed together in a mortar, then the mixture was packed firmly into the cavity of the teflon holder (3.0 mm in diameter) and the electrical contact was established via a copper wire. A new surface was obtained by smoothing the electrode onto a piece of weighing paper. The prepared electrode was denoted as N-GE/nano-CPE.

For comparison, traditional carbon paste electrode (CPE) was made up of common graphite powder and paraffin oils. Nano-carbon paste electrode (nano-CPE) was prepared using nano-graphite powder instead of common graphite powder. Plain graphene modified nano-carbon paste electrode (GE/nano-CPE) was prepared by mixing nano-graphite powder, plain graphene, and paraffin oil. When not in use, the modified electrodes were kept in room temperature with a cover to protect them from dust.

### Analytical procedure

Electrochemical measurements were performed in 0.2 M acetate buffer containing various concentrations of  $\text{Pb}^{2+}$  and  $\text{Cd}^{2+}$  using square wave anodic stripping voltammetry (SWASV). Firstly, the pre-concentration step was carried out in a stirred solution at the potential of  $-1.0$  V for 210 s. After a

quiet time of 2 s, and the voltammograms were recorded from  $-1.0$  V to  $-0.2$  V with step potential 4 mV, pulse amplitude 30 mV and frequency 15 Hz. After each measurement the modified electrode was regenerated at potential of 0.0 V for 60 s in order to remove the residual deposits.

## Results and discussion

### Choice of materials

Carbon-based nanomaterials have widely applied in the construction of electrochemical sensors, such as multi-walled carbon nanotubes (MWCNTs), graphene (GE) and their derivatives. Compared to MWCNTs, graphene exhibits increased electron transfer ability and enlarged surface area. Nitrogen-doped graphene (N-GE) is derived from graphene. In comparison with graphene, enhancement of the electrocatalytic activity and the conductivity is found in N-GE due to the doping of nitrogen. This is because the doped nitrogen atoms can increase active sites for electrocatalysis. Nitrogen atom contains five valence electrons, and it can form strong valence bonds with carbon atoms. The distribution of electrons changes and free electrons are introduced when nitrogen is doped into the graphene structure [13]. Therefore, we chose the N-GE as modifier due to its superior performance. The results indicated that the current responses of  $\text{Cd}^{2+}$  and  $\text{Pb}^{2+}$  increased obviously on the N-GE/nano-CPE compared to those on the GE/nano-CPE.

### Electrochemical characterization of of the modified electrode

Figure 1a shows cyclic voltammograms of different electrodes in 1 mM  $[\text{Fe}(\text{CN})_6]^{3-/4-}$  solution containing 0.1 M KCl. As seen in the figure, the peak potential separations ( $\Delta E_p$ ) were: CPE > nano-CPE > N-GE/nano-CPE, and the peak currents ( $I_p$ ) were: CPE < nano-CPE < N-GE/nano-CPE. A pair of weak redox peaks with the largest  $\Delta E_p$  was observed on CPE (curve a) due to the poor conductivity of paraffin oil, indicating the slow electron transfer rate at the interface. By using the nano-CPE (curve b), well-defined and enhanced redox peaks with smaller  $\Delta E_p$  were obtained. This is ascribed to the nano-structure and excellent electrocatalytic activity of nano-graphite powder. Compared with CPE and nano-CPE, the highest peak currents and the smallest  $\Delta E_p$  were observed on N-GE/nano-CPE (curve c) due to the large surface area and good conductivity of N-GE.

Electrochemical impedance spectroscopy (EIS) was further utilized to investigate the properties of different modified electrodes. The typical impedance spectrum is made up of a semicircle portion at higher frequencies indicating electron transfer process, and a linear portion at lower frequencies corresponding to the diffusion process. The charge transfer resistance (Rct)

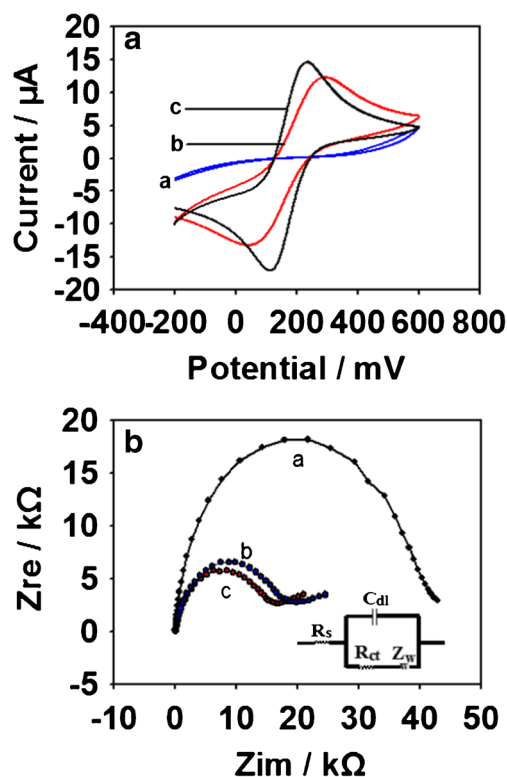


**Fig. 1** a Cyclic voltammograms (scan rate:  $50 \text{ mV s}^{-1}$ ) and b Nyquist plots (frequency:  $0.1\text{--}10^5$  Hz) of different electrodes in 1 mM  $[\text{Fe}(\text{CN})_6]^{3-/4-}$  solution containing 0.1 M KCl: a CPE; b nano-CPE; c N-GE/nano-CPE. The insert: the equivalent circuit

value is calculated by measuring the diameter of the high-frequency semicircle in the Nyquist plots. In addition, an equivalent circuit consists of the ohmic resistance of the electrolyte ( $R_s$ ), the charge transfer resistance ( $R_{ct}$ ), the Warburg impedance ( $Z_w$ ), and interfacial capacitance ( $C_{dl}$ ). Figure 1b depicts the Nyquist diagrams of the different modified electrodes. By fitting the equivalent circuit (the inset of Fig. 1b), the  $R_{ct}$  value at the CPE (curve a) was obtained as  $39.28 \pm 1.83 \text{ k}\Omega$ , indicating a very high electron transfer resistance. This is attributed to the poor conductivity of paraffin oil. The  $R_{ct}$  value ( $19.66 \pm 0.74 \text{ k}\Omega$ ) of the nano-CPE (curve b) remarkably decreased. This indicates that the use of nano-CPE accelerates the electron transfer between redox probe and electrode. The  $R_{ct}$  value ( $16.27 \pm 0.67 \text{ k}\Omega$ ) of N-GE/nano-CPE (curve c) further decreased due to the good conductivity and large surface area of N-GE. This exhibits that the N-GE modified electrode possesses excellent electron transport ability. The impedance changes of the modified electrode also indicated that N-GE was successfully modified on the surface of nano-CPE.

### Electrode surface area

The effective surface areas of nano-CPE and N-GE/nano-CPE were investigated by cyclic voltammetry at different scan rates in 5 mM  $[\text{Fe}(\text{CN})_6]^{3-/4-}$  solution containing 0.1 M KCl, and

the results were shown in Fig. 2. When gradually increasing the scan rate from 25 to 200  $\text{mV s}^{-1}$ , the peak currents linearly increased with the square root of scan rate. For a reversible process, the function of anodic peak current ( $I_p$ , A) versus the square root of scan rate ( $\nu$ ,  $\text{V s}^{-1}$ ) can be expressed by Randles-Sevcik equation [16]:

$$I_p = (2.69 \times 10^5) n^{3/2} A C_0 D_R^{1/2} \nu^{1/2} \quad (1)$$

where  $n$  is the electron transfer number,  $A$  is effective surface area of the electrode ( $\text{cm}^2$ ),  $C_0$  is the concentration for  $\text{K}_3[\text{Fe}(\text{CN})_6]$  ( $\text{mol L}^{-1}$ ) and  $D_R$  is the diffusion coefficient of  $\text{K}_3[\text{Fe}(\text{CN})_6]$  ( $\text{cm}^2 \text{s}^{-1}$ ). For  $\text{K}_3[\text{Fe}(\text{CN})_6]$ ,  $n = 1$ ,  $D_R = 7.60 \times 10^{-6} \text{ cm}^2 \text{ s}^{-1}$ . From the slope of the  $I_p$ - $\nu^{1/2}$  relation, the electrochemical active area of N-GE/nano-CPE and nano-CPE were calculated to be  $0.073 \pm 0.003 \text{ cm}^2$  and  $0.051 \pm 0.002 \text{ cm}^2$ , respectively. This indicated that the active area of the N-GE/nano-CPE increased significantly and was about 1.4 times larger than that of the nano-CPE.

### Electrochemical response of lead(II) and cadmium(II)

Figure 3 shows the square wave anodic stripping voltammograms of  $1 \mu\text{M Pb}^{2+}$  and  $1 \mu\text{M Cd}^{2+}$  on different electrodes. Two weak stripping peaks for  $\text{Cd}^{2+}$  ( $0.34 \mu\text{A}$ ) and  $\text{Pb}^{2+}$

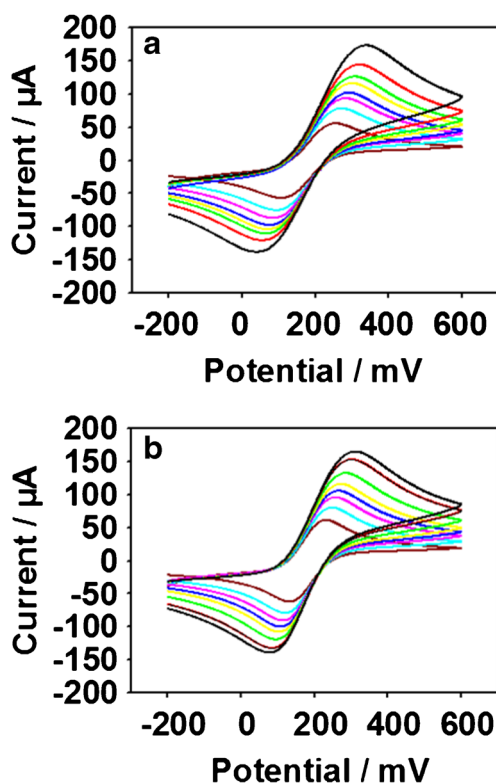


**Fig. 2** Cyclic voltammograms of **a** nano-CPE; **b** N-GE/nano-CPE with different scan rate in  $5 \text{ mM Fe}(\text{CN})_6^{3-/4-}$  solution containing  $0.1 \text{ M KCl}$ , scan rates (from inner to outer): 25, 50, 75, 100, 125, 150, 175,  $200 \text{ mV s}^{-1}$

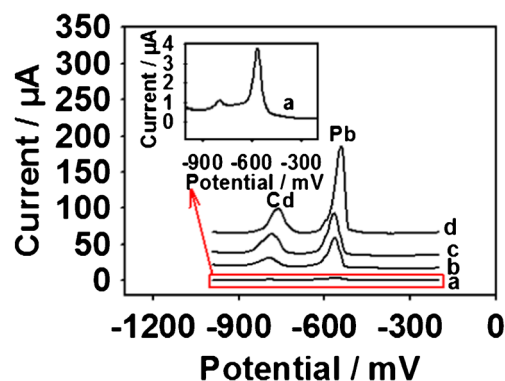


**Fig. 3** SWASV responses of  $1 \mu\text{M Cd}^{2+}$  and  $1 \mu\text{M Pb}^{2+}$  at **a** CPE; **b** nano-CPE; **c** GE/nano-CPE; **d** N-GE/nano-CPE in  $0.2 \text{ M acetate buffer (pH 5.0)}$ . The inset: The amplification of CPE (**a**). Deposition potential:  $-1.0 \text{ V}$ , deposition time:  $210 \text{ s}$

( $3.27 \mu\text{A}$ ) were observed on the CPE (Curve a). The response signals on the nano-CPE (Curve b) were nearly 35 times and 13 times larger for  $\text{Cd}^{2+}$  and  $\text{Pb}^{2+}$  than those obtained on the CPE, respectively. This exhibits that nano-CPE promotes the accumulation of  $\text{Cd}^{2+}$  and  $\text{Pb}^{2+}$  on the electrode surface and shows good electrocatalytic activities. Compared to nano-CPE, an enhancement of current responses of about 130 % and 42 % for  $\text{Cd}^{2+}$  and  $\text{Pb}^{2+}$  was obtained on the GE/nano-CPE (Curve c), respectively. The current responses of  $\text{Cd}^{2+}$  and  $\text{Pb}^{2+}$  further increased for about 26 % and 107 % on the N-GE/nano-CPE compared to those on GE/nano-CPE, respectively. This phenomenon can be explained by the following reasons: On one hand, the modifier N-GE with good conductivity can promote electron transfer of lead and cadmium, and more ions can be deposited on the surface of the electrode in shorter time; On the other hand, N-GE possesses large surface area, and the doped nitrogen atoms can provide more active sites for electrocatalysis of heavy metals, which improves the sensitivity of the modified electrode.

### Optimization of method

The following parameters were optimized: (a) Sample pH value; (b) Amount of modifier; (c); Deposition time (d) Deposition potential. Respective data and Figures are given in the [Electronic Supporting Material](#). The following experimental conditions were found to give best results: (a) A sample pH value of 5.0; (b) 2.5 % of N-GE in carbon paste; (c) Deposition time of 210 s; (d) Deposition potential of  $-1.0 \text{ V}$ .

### Determination of lead(II) and cadmium(II)

Figure 4 presents the square wave anodic stripping voltammograms of different concentrations of  $\text{Cd}^{2+}$  and  $\text{Pb}^{2+}$  in  $0.2 \text{ M acetate buffer (pH 5.0)}$  under the optimal conditions. Two sharp and well-defined stripping peaks occurred at potentials of about  $-0.77 \text{ V}$  for  $\text{Cd}^{2+}$  and about  $-0.56 \text{ V}$  for  $\text{Pb}^{2+}$ ,



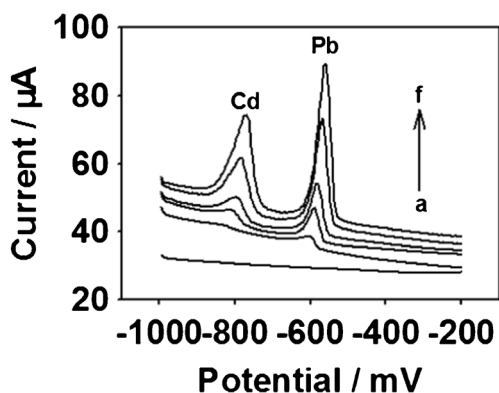


**Fig. 4** SWASVs for different concentrations of  $\text{Cd}^{2+}$  and  $\text{Pb}^{2+}$  at N-GE/nano-CPE (from a to i: 0, 0.01, 0.05, 0.1, 0.5, and 1 nM). Deposition potential: -1.0 V, deposition time: 210 s

respectively. The peak currents of  $\text{Cd}^{2+}$  and  $\text{Pb}^{2+}$  exhibited excellent linear dependence on their corresponding concentrations in the range from  $1 \times 10^{-11}$  M to  $1 \times 10^{-9}$  M, and the linear regression equations were:  $I(\mu\text{A}) = 41.8463 c (\text{nM}) + 7.1534$  ( $r^2 = 0.9920$ ) for  $\text{Pb}^{2+}$  and  $I(\mu\text{A}) = 24.3859 c (\text{nM}) + 1.5889$  ( $r^2 = 0.9904$ ) for  $\text{Cd}^{2+}$ , respectively. The detection limits at signal to noise ratio of 3 were  $5 \times 10^{-12}$  M for  $\text{Pb}^{2+}$  and  $8 \times 10^{-12}$  M for  $\text{Cd}^{2+}$ , respectively.

A comparison of the N-GE/nano-CPE with other reported modified electrodes [17–21] for the determination of  $\text{Cd}^{2+}$  and  $\text{Pb}^{2+}$  is listed in Table 1. The method exhibits comparative or even better linear range and detection limit. Moreover, the modified electrode has the advantages of simple preparation, ease of renewable surface, and convenient operation.

### Reproducibility and stability

The reproducibility of the modified electrode was evaluated by repetitive measurement of  $0.5 \mu\text{M}$   $\text{Pb}^{2+}$  and  $0.5 \mu\text{M}$   $\text{Cd}^{2+}$ . For one electrode, the relative standard deviation (R.S.D.) was 3.4 % for  $\text{Cd}^{2+}$  and 3.7 % for  $\text{Pb}^{2+}$  in six times measurements. For six different electrodes prepared in the same procedure,

the R.S.D. was 4.1 % for  $\text{Cd}^{2+}$  and 4.5 % for  $\text{Pb}^{2+}$ , respectively. The storage stability of the sensor was also studied. The electrode remained about 94.5 % and 95.3 % of the original responses for  $\text{Cd}^{2+}$  and  $\text{Pb}^{2+}$  after its storage at ambient conditions for three weeks. These results indicate that the sensor can be successfully applied to the simultaneous determination of heavy metal ions with excellent repeatability and stability.

### Potentially interfering ions

The effect of various cations and anions on the simultaneous determination of  $\text{Pb}^{2+}$  and  $\text{Cd}^{2+}$  was investigated. The results exhibited that 1000-fold  $\text{Na}^+$ ,  $\text{K}^+$ ,  $\text{Ca}^{2+}$ ,  $\text{Ba}^{2+}$ ,  $\text{Mg}^{2+}$ ,  $\text{Mn}^{2+}$ ,  $\text{Zn}^{2+}$ ,  $\text{Al}^{3+}$ ,  $\text{Fe}^{3+}$ ,  $\text{Cr}^{3+}$ ,  $\text{Cl}^-$ ,  $\text{NO}_3^-$ ,  $\text{SCN}^-$ ,  $\text{CO}_3^{2-}$ ,  $\text{SO}_4^{2-}$ ,  $\text{PO}_4^{3-}$  had no significant effect on the signals of  $\text{Pb}^{2+}$  and  $\text{Cd}^{2+}$  (tolerated ratios:  $\leq \pm 5.0$  %). 100-fold  $\text{Cu}^{2+}$  was found to have a large influence on the stripping responses of target ions, peak currents of  $\text{Pb}^{2+}$  and  $\text{Cd}^{2+}$  decreased remarkably. This suppression effect was probably ascribed to the competition between copper and target ions on the electrode surface. The interference of copper can be eliminated by ferrocyanide in the form of a stable and insoluble copper-ferrocyanide complex [22]. In addition, 100-fold  $\text{Hg}^{2+}$  increased the stripping responses significantly. This is attributed to the formation of mercury film at the modified electrode surface, which promotes the reduction of  $\text{Cd}^{2+}$  and  $\text{Pb}^{2+}$  by forming amalgam [23]. Therefore, most common ions did not interfere with the determination and the sensor exhibited good selectivity.

### Analysis applications

To evaluate the feasibility of the modified electrode for practical analysis, the N-GE/nano-CPE was applied to detect  $\text{Cd}^{2+}$  and  $\text{Pb}^{2+}$  in real water samples. A certain volume of lake water samples were added in 0.2 M acetate buffer and no further sample treatment was done. Table 2 illustrates the results obtained for the water samples using standard addition method.

**Table 1** Comparison of different electrodes for the determination of  $\text{Pb}^{2+}$  and  $\text{Cd}^{2+}$

Electrodes	Method	Linear range $\text{Cd}^{2+}/\text{M}$	Linear range $\text{Pb}^{2+}/\text{M}$	Detection limit $\text{Cd}^{2+}/\text{M}$	Detection limit $\text{Pb}^{2+}/\text{M}$	References
G-Sn/GCS electrode	SWASV	$1.0 \times 10^{-8}$ – $1.0 \times 10^{-7}$	$1.0 \times 10^{-8}$ – $1.0 \times 10^{-7}$	$6.3 \times 10^{-10}$	$6.0 \times 10^{-10}$	[17]
Cupferron and $\beta$ -naphthol/MWCNTs/GCE	DPV	$5.0 \times 10^{-11}$ – $1.6 \times 10^{-8}$ , $1.6 \times 10^{-8}$ – $1.42 \times 10^{-6}$	–	$1.6 \times 10^{-11}$	–	[18]
Bismuth film electrode	SWASV	$2.0 \times 10^{-10}$ – $5.0 \times 10^{-9}$	$5.0 \times 10^{-10}$ – $5.0 \times 10^{-9}$	$4.5 \times 10^{-11}$	$1.8 \times 10^{-10}$	[19]
PANI-MES/OMC/GCE	DPASV	$1.0 \times 10^{-9}$ – $1.2 \times 10^{-7}$	$1.0 \times 10^{-9}$ – $1.2 \times 10^{-7}$	$2.6 \times 10^{-10}$	$1.6 \times 10^{-10}$	[20]
C polyL	DPASV	$4.0 \times 10^{-8}$ – $1.0 \times 10^{-6}$	$1.0 \times 10^{-9}$ – $1.0 \times 10^{-7}$	$1.0 \times 10^{-8}$	$7.0 \times 10^{-10}$	[21]
N-GE/nano-CPE	SWASV	$1 \times 10^{-11}$ – $1 \times 10^{-9}$	$1 \times 10^{-11}$ – $1 \times 10^{-9}$	$8.0 \times 10^{-12}$	$5.0 \times 10^{-12}$	This work

G-Sn reduced graphene oxide decorated with tin nanoparticles, GCS glassy carbon sheet, SWASV square wave anodic stripping voltammetry, MWCNTs multiwalled carbon nanotubes, GCE glassy carbon electrode, DPV differential pulse voltammetry, PANI tethered polyaniline, MES 2-mercaptoethanesulfonate, OMC ordered mesoporous carbon, DPASV differential pulse anodic stripping voltammetry, L 4-azulen-1-yl-2,6-bis(2-thienyl)pyridine, C glassy carbon electrode, N-GE nitrogen doped graphene, nano-CPE nano-carbon paste electrode

**Table 2** Determination of Pb<sup>2+</sup> and Cd<sup>2+</sup> in real samples using N-GE/nano-CPE (*n* = 3<sup>a</sup>)

Sample	Spiked (pM)		Detected (pM)		Recovery (%)		RSD (%)	
	Pb <sup>2+</sup>	Cd <sup>2+</sup>	Pb <sup>2+</sup>	Cd <sup>2+</sup>	Pb <sup>2+</sup>	Cd <sup>2+</sup>	Pb <sup>2+</sup>	Cd <sup>2+</sup>
1	100.0	100.0	98.2	95.3	98.2	95.3	3.52	4.31
2	500.0	500.0	479.3	485.7	95.9	97.1	2.71	3.94

<sup>a</sup> Mean of three determinations

The results are satisfying and indicate that this is an effective method for the simultaneously determination of Pb<sup>2+</sup> and Cd<sup>2+</sup> in practical samples.

## Conclusions

Simultaneous determination of cadmium and lead at trace levels by SWASV was firstly carried out on the N-GE/nano-CPE with high sensitivity. The N-GE/nano-CPE exhibited better enrichment ability and excellent electron transfer for lead and cadmium due to large surface area and good conductivity of N-GE. The fabricated electrode had the advantages of simple preparation, ease of renewable surface, as well as low cost, which was expected to be applied in environmental monitoring.

**Acknowledgments** This research was supported by Ningxia Medical University Scientific Research Project (No. XM201415 and No. XZ2015002).

## References

- Viyannalage LT, Bliznakov S, Dimitrov N (2008) Electrochemical method for quantitative determination of trace amounts of lead. *Anal Chem* 80:2042–2049
- Nguyen PKQ, Lunsford SK (2013) Square wave anodic stripping voltammetric analysis of lead and cadmium utilizing titanium dioxide/zirconium dioxide carbon paste composite electrode. *J Electroanal Chem* 711:45–52
- Wang ZQ, Wang H, Zhang ZH, Liu G (2014) Electrochemical determination of lead and cadmium in rice by a disposable bismuth/electrochemically reduced graphene/ionic liquid composite modified screen-printed electrode. *Sensors Actuators B* 199:7–14
- Gasparik J, Vladořova D, Capcarova M, Smehyl P, Slamecka J, Garaj P, Stawarz R, Massanyi P (2010) Concentration of lead, cadmium, mercury and arsenic in leg skeletal muscles of three species of wild birds. *J Environ Sci Health A* 45:818–823
- Pohl P (2009) Determination of metal content in honey by atomic absorption and emission spectrometry. *TrAC Trends Anal Chem* 28:117–128
- Sen I, Shandil A, Shrivastava VS (2011) Study for determination of heavy metals in fish species of the river Yamuna (Delhi) by inductively coupled plasma-optical emission spectroscopy (ICP-OES). *Adv Appl Sci Res* 2:161–166
- Kempegowda RG, Malingappa P (2012) A binderless, covalently bulk modified electrochemical sensor: application to simultaneous determination of lead and cadmium at trace level. *Anal Chim Acta* 728:9–17
- Promphet N, Rattanarat P, Rangkupan R, Chailapakul O, Rodthongkum N (2015) An electrochemical sensor based on graphene/polyaniline/polystyrene nanoporous fibers modified electrode for simultaneous determination of lead and cadmium. *Sensors Actuators B* 207:526–534
- Kuila T, Bose S, Khanra P, Mishra AK, Kim NH, Lee JH (2011) Recent advances in graphene-based biosensors. *Biosens Bioelectron* 26:4637–4648
- Sookhakian M, Amin Y, Baradaran S, Tajabadi M, Golsheikh AM, Basirun W (2014) A layer-by-layer assembled graphene/zinc sulfide/polypyrrole thin-film electrode via electrophoretic deposition for solar cells. *Thin Solid Films* 552:204–211
- Xu HY, Xiao JJ, Liu BH, Griveau S, Bedioui F (2015) Enhanced electrochemical sensing of thiols based on cobalt phthalocyanine immobilized on nitrogen-doped graphene. *Biosens Bioelectron* 66:438–444
- Tian Y, Wang FL, Liu YX, Pang F, Zhang X (2014) Green synthesis of silver nanoparticles on nitrogen-doped graphene for hydrogen peroxide detection. *Electrochim Acta* 146:646–653
- Shi LB, Niu XH, Liu TT, Zhao HL, Lan MB (2015) Electrocatalytic sensing of hydrogen peroxide using a screen printed carbon electrode modified with nitrogen-doped graphene nanoribbons. *Microchim Acta* 182:2485–2493
- Giribabu K, Suresh R, Manigandan R, Kumar SP, Muthamizh S, Munusamy S, Narayanan V (2014) Preparation of nitrogen-doped reduced graphene oxide and its use in a glassy carbon electrode for sensing 4-nitrophenol at nanomolar levels. *Microchim Acta* 181:1863–1870
- Tsierkezos NG, Szroeder P, Ritter U (2014) Voltammetric study on pristine and nitrogen-doped multi-walled carbon nanotubes decorated with gold nanoparticles. *Microchim Acta* 181:329–337
- Li YH, Zhai XR, Wang HB, Liu XS, Guo L, Ji XL, Wang L, Qiu HY, Liu XY (2015) Non-enzymatic sensing of uric acid using a carbon nanotube ionic-liquid paste electrode modified with poly( $\beta$ -cyclodextrin). *Microchim Acta* 182:1877–1884
- Lee PM, Chen Z, Li L, Liu E (2015) Reduced graphene oxide decorated with tin nanoparticles through electrodeposition for simultaneous determination of trace heavy metals. *Electrochim Acta* 174:207–214
- Liu M, Feng YH, Wang GF, Fang B (2012) Determination of cadmium(II) using glassy carbon electrodes modified with cupferron,  $\beta$ -naphthol, and multiwalled carbon nanotubes. *Microchim Acta* 177:221–228
- Rutyna I, Korolczuk M (2014) Determination of lead and cadmium by anodic stripping voltammetry at bismuth film electrodes following double deposition and stripping steps. *Sensors Actuators B* 204:136–141
- Tang L, Chen J, Zeng GM, Zhu Y, Zhang Y, Zhou YY, Xie X, Yang GD, Zhang S (2014) Ordered mesoporous carbon and thiolated polyaniline modified electrode for simultaneous determination of cadmium(II) and lead(II) by anodic stripping voltammetry. *Electroanalysis* 26:2283–2291
- Buica GO, Ungureanu EM, Birzan L, Razus AC, Mandoc (Popescu) LR (2013) Voltammetric sensing of lead and cadmium using poly(4-azulen-1-yl-2,6-bis(2-thienyl)pyridine) complexing films. *J Electroanal Chem* 693:67–72
- Ping JF, Wang YX, Wu J, Ying YB (2014) Development of an electrochemically reduced graphene oxide modified disposable bismuth film electrode and its application for stripping analysis of heavy metals in milk. *Food Chem* 151:65–71
- Li YH, Liu XY, Zeng XD, Liu Y, Liu XT, Wei WZ, Luo SL (2009) Simultaneous determination of ultra-trace lead and cadmium at a hydroxyapatite-modified carbon ionic liquid electrode by square-wave stripping voltammetry. *Sensors Actuators B* 139:604–610